



# Density Functional Theory investigation of guanosine triphosphate models Catalytic role of $Mg^{2+}$ ions in phosphate ester hydrolysis

Elena Franzini, Piercarlo Fantucci, Luca De Gioia\*

*University of Milan-Bicocca, Piazza della Scienza 2, I-20126 Milan, Italy*

Received 19 September 2002; received in revised form 25 March 2003; accepted 28 March 2003

Dedicated to Professor Renato Ugo on occasion of his 65th birthday, in recognition of his constant and stimulating interest for the theoretical aspects of homogeneous catalysis

## Abstract

Hydrolysis of phosphate ester bonds is a key reaction in biological systems and many enzymes require one or more metal ions as cofactors to catalyse this reaction. However, the exact role of metal ions is still unclear. In this contribution, we have investigated the influence of  $Mg^{2+}$  on the hydrolysis of guanosine triphosphate (GTP) models using Density Functional Theory (DFT).

Results indicate that  $Mg^{2+}$  catalyses phosphate ester hydrolysis, stabilizing the transition state (TS) both for associative and dissociative pathways. In the associative pathway, the reaction is promoted by an increased electrophilicity of the reactive phosphorus atom, whereas in the dissociative pathway catalysis is achieved by stabilization of  $\beta$ -phosphate due to  $Mg^{2+}$  coordination. Considering relative energy values, it turns out that the dissociative pathway is more favorable.

© 2003 Elsevier Science B.V. All rights reserved.

*Keywords:* Density Functional Theory; Phosphate hydrolysis; Enzyme models; Ras protein; Reaction mechanism

## 1. Introduction

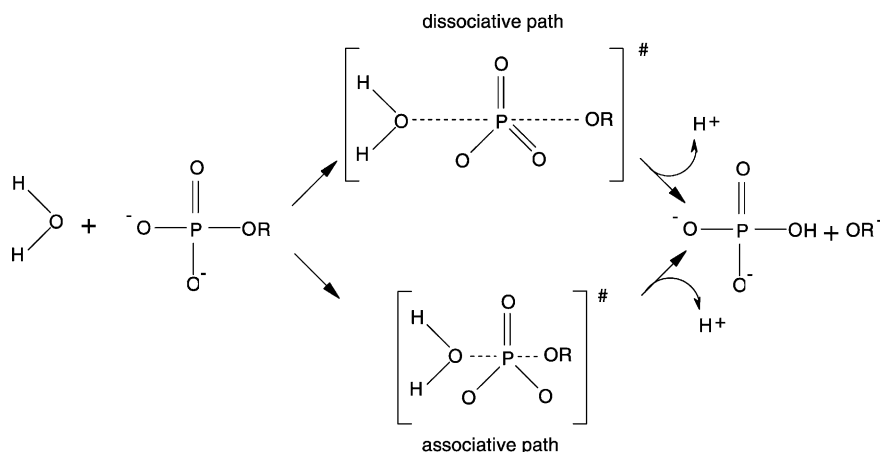
The cleavage of phosphate ester bonds is an essential reaction in biological systems [1] and the investigation of its reaction mechanism in aqueous solution has been the subject of great experimental ([2] and references therein) and theoretical ([3–6] and references therein) efforts. The reactions that lead to the cleavage of the phosphoester bond can be divided in two major classes: a dissociative path, which proceeds via the hydrated metaphosphate ion  $PO_3^-$ , and an asso-

ciative path, which requires the formation of an intermediate or transition state (TS) with five-coordinated phosphorous (see Scheme 1).

Among the enzymes involved in phosphoester bond cleavage, Ras has great biological relevance, playing a central role in the proliferation processes of the cell [7]. In fact, this protein has become known as Ras because the gene encoding for it was originally isolated from rats with sarcoma. In particular, Ras acts as a molecular switch, which is bound to guanosine triphosphate (GTP) and guanosine diphosphate (GDP) in its “on” and “off” states, respectively. The X-ray structure of Ras in its active and inactive form [8] reveals the presence of a  $Mg^{2+}$  ion in the active site.

\* Corresponding author. Fax: +39-02-64483478.

E-mail address: [luca.degioia@unimib.it](mailto:luca.degioia@unimib.it) (L. De Gioia).



Scheme 1. Limit reaction mechanisms of phosphate ester hydrolysis.

In Ras-GTP, the  $\text{Mg}^{2+}$  ion is octahedrally coordinated by two oxygen atoms belonging respectively to  $\beta$ - and  $\gamma$ -phosphate, by the side chains of Ser17 and Thr35 and by two  $\text{H}_2\text{O}$  molecules. In the X-ray structure of Ras-GDP, the  $\beta$ -phosphate group interacts extensively with the protein and is coordinated to  $\text{Mg}^{2+}$ , whereas  $\alpha$ -phosphate does not interact with the metal ion.

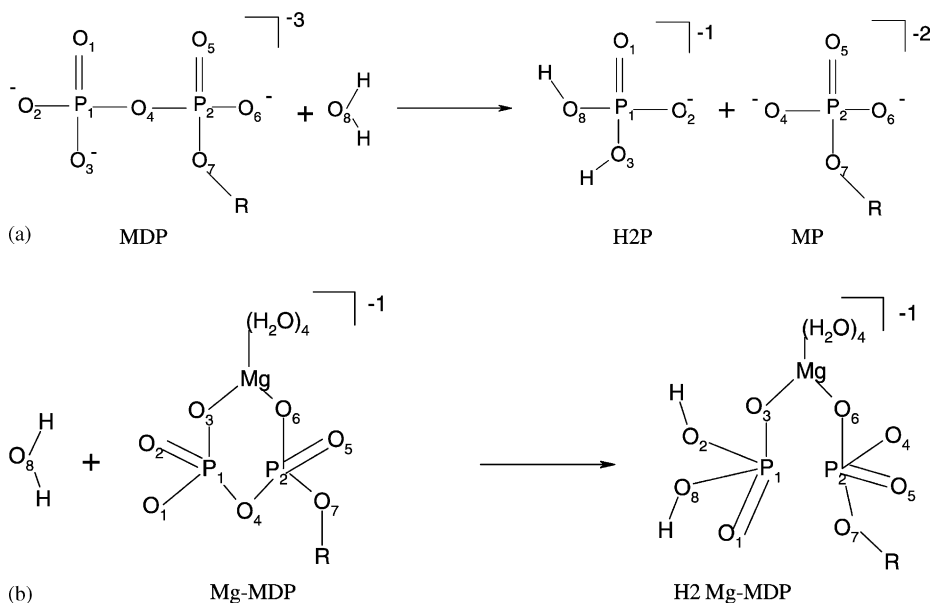
As a matter of fact, many enzymes require one or more metal ions as cofactors to catalyse phosphate ester hydrolysis. However, despite a large knowledge base of metallo-enzyme crystal structures, kinetic and binding data, and extensive studies with model systems, the detailed role of metal ions is still unclear [9,10]. In particular, the issue has been raised whether the metal ions stabilize the transition state of the uncatalyzed reaction, or a significantly different transition state. Recently, the catalytic role of  $\text{Mg}^{2+}$  ions in adenosine triphosphate hydrolysis have been established experimentally investigating tailored-made model systems [11]. However, little is known about the possible catalytic role of  $\text{Mg}^{2+}$  in Ras.

In this contribution, we have investigated hydrolysis of GTP models by means of Density Functional Theory (DFT) calculations, with the aim of characterizing the reaction path and clarify the role of  $\text{Mg}^{2+}$  in catalysis. To carry out high quality DFT calculations, GTP had to be modeled by a simpler analogous still maintaining crucial structural and electronic features.

In particular, the guanosine monophosphate (GMP) moiety, which is expected to play a marginal role in the hydrolysis of the  $\gamma$ -phosphate ester bond, was replaced by a methyl group. In spite of the adopted simplifications, it should be noted that this is presently the largest GTP model investigated by quantum chemical approaches for which energy minima and saddle point structures have been reported. Moreover, to investigate also the role of the solvent, we have studied reactions both in vacuum and in water solution, modeling bulk solvent by means of the polarizable continuum model (PCM) method [12].

## 2. Methods

DFT calculations have been carried out using the hybrid B3LYP exchange-correlation functional [13–16] and the 6–31+G\*\* basis set, which was shown to be well suited to investigate this class of compounds [17]. Stationary points of the energy hypersurface have been located by means of energy gradient techniques. In particular, transition state structures have been optimized using the Synchronous Transit Quasi-Newton method [18], as implemented in the Gaussian98 set of programs [19]. A full vibrational analysis has been carried out to characterize each stationary point. The intrinsic reaction coordinate (IRC) was calculated as steepest descent path on the electronic enthalpy surface that connects reactants and transition state.



Scheme 2. Schematic representation of the reaction step investigated in the present contribution. The guanosine monophosphate moiety of GTP has been modeled as a methyl group (R). Relevant atoms are numbered for the sake of clarity (see text and tables). (a) MDP-H<sub>2</sub>P-MP (b) Mg-MDP-H<sub>2</sub>Mg-MDP.

Aqueous solution effects were estimated according to the PCM method [12], as implemented in Gaussian98, using the default Pauling atomic radii to define the cavity. The protonation state of the models was chosen according to the  $pK_a$  value of GTP and pyrophosphate [20]; at physiological pH (7.4) both GTP and the model species methyl-pyrophosphate (MDP) are predominantly present in their fully deprotonated forms. A methyl group instead of a hydrogen atom was chosen to substitute the GMP group, to avoid formation of fictitious hydrogen-bonds. It should be noted that, according to the simplifications that had to be adopted in the present study, the  $\beta$ - and  $\gamma$ -phosphate groups of GTP correspond to the  $\alpha$ - and  $\beta$ -phosphate groups of methyl-pyrophosphate, respectively. The  $Mg^{2+}$  coordination geometry and GTP arrangement observed in Ras active site have been used as reference, substituting Ser17 and Thr35 side chains with two  $H_2O$  molecules. The  $Mg^{2+}$  six-coordination has been completed by other two  $H_2O$  molecules. For the sake of clarity, atoms referred in the text and tables are numbered according to Scheme 2.

### 3. Results

The X-ray structures of Ras-GTP and Ras-GDP [8] have been extremely important to understand several aspects of GTP hydrolysis and binding. However, even though previous investigations proved that, in the enzymatic system, the reactive water molecule attacks the  $\gamma$ -phosphate group [8], a general consensus about the reaction mechanism has not been reached. In fact, water is generally not considered to be nucleophilic enough (assuming an associative mechanism) and a general base is thought to be needed to activate it. Analysis of Ras structure suggested that Gln61 might be a suitable candidate as general base [21,22]. However, the low  $pK$  value of this group disfavors this hypothesis. Another likely general base might be the  $\gamma$ -phosphate itself, according to a mechanism that has been called substrate assisted catalysis [23,24], even though this view has been very recently challenged [6]. Moreover, both associative and dissociative mechanisms have been proposed for this reaction step [25]. To clarify some of these aspects and to obtain reference data to evaluate the role of  $Mg^{2+}$  in promoting

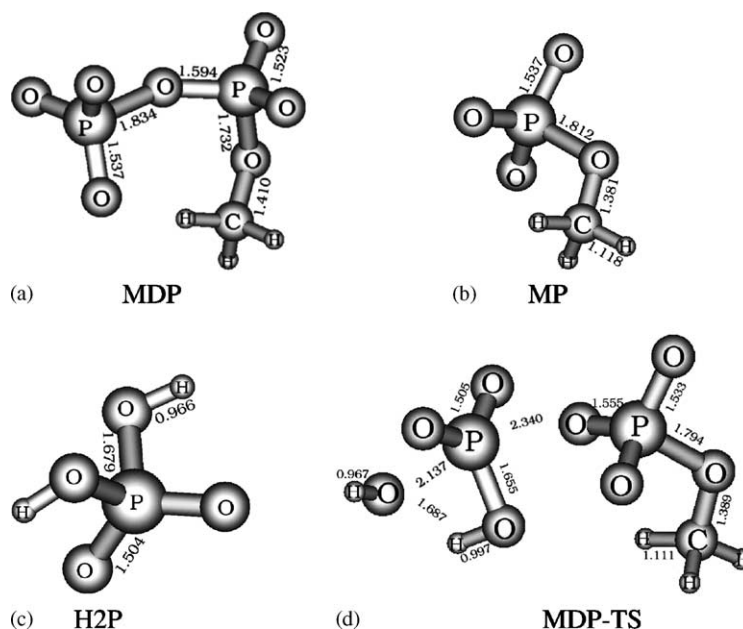


Fig. 1. DFT optimized structures of MDP, MP, H2P and MDP-TS. Relevant bond distances (in angstrom) are shown.

GTP hydrolysis, we have initially investigated this reaction in absence of metal ions (see Scheme 2a). In particular, we have investigated the hydrolysis of the model compound methyl-pyrophosphate, leading to methyl-phosphate (MP) and di-hydrogen-phosphate (H2P) as initial products. The optimized structures of MDP, MP and H2P are shown in Fig. 1.

In MDP, due to its asymmetric electrostatic environment, the oxygen atom bridging the two phosphate groups is closer to P2 ( $P2-O4 = 1.594 \text{ \AA}$ ) than to P1 ( $P1-O4 = 1.834 \text{ \AA}$ ), in agreement with similar observations reported for pyrophosphate derivatives [17]. Moreover, the long  $P1-O4$  distance indicates a relatively weak bond.

Considering reaction products, in H2P the  $P-OH$  distances are equal to  $1.679 \text{ \AA}$ , whereas the  $P-O$  distances are smaller ( $1.504 \text{ \AA}$ ), as expected considering the higher bond order. In MP, the  $P-O$  distances are slightly longer than those computed for H2P ( $1.537 \text{ \AA}$  versus  $1.504 \text{ \AA}$ ), whereas the  $P-OCH_3$  bond distance is larger than the corresponding  $P-OH$  distance observed in H2P ( $1.812 \text{ \AA}$  versus  $1.679 \text{ \AA}$ ).

Then, we have searched for transition state structures along the reaction path  $MDP + H_2O \rightarrow MP + H_2P$ . In the computed transition state (MDP-TS,

see Fig. 1d) the terminal phosphate has a trigonal planar geometry, as indicated by the dihedral angle  $P1-O1-O2-O3$  ( $-0.56^\circ$ ), whereas the leaving group remains tetrahedral. Remarkably, MDP-TS cannot be classified neither as a purely associative nor dissociative transition state. The  $P1-O4$  distance is large enough ( $2.340 \text{ \AA}$  in MDP-TS versus  $1.834 \text{ \AA}$  in MDP) to suggest a dissociative mechanism. However, the reacting water molecule participates to the formation of the transition state ( $P1-O8 = 2.137 \text{ \AA}$ ). To supplement these data, we have computed the IRC going from reactants to transition state for the  $MDP + H_2O \rightarrow MP + H_2P$  reaction. The variation of relevant bond lengths along the IRC is reported in Fig. 2, indicating that proton transfer from water to terminal phosphate and  $OH^-$  nucleophilic attack are concerted. In addition, no evidence was found for the existence of a reaction intermediate. Considering relative energy values, it turns out that the reaction energy computed in vacuum is extremely favorable ( $-136.6 \text{ kcal mol}^{-1}$ ). This is not surprising considering that the large negative charge of reactants ( $-3$ ) is well delocalized in the products. Indeed, the situation is drastically changed when solvation effects are considered: the reaction energy is reduced to

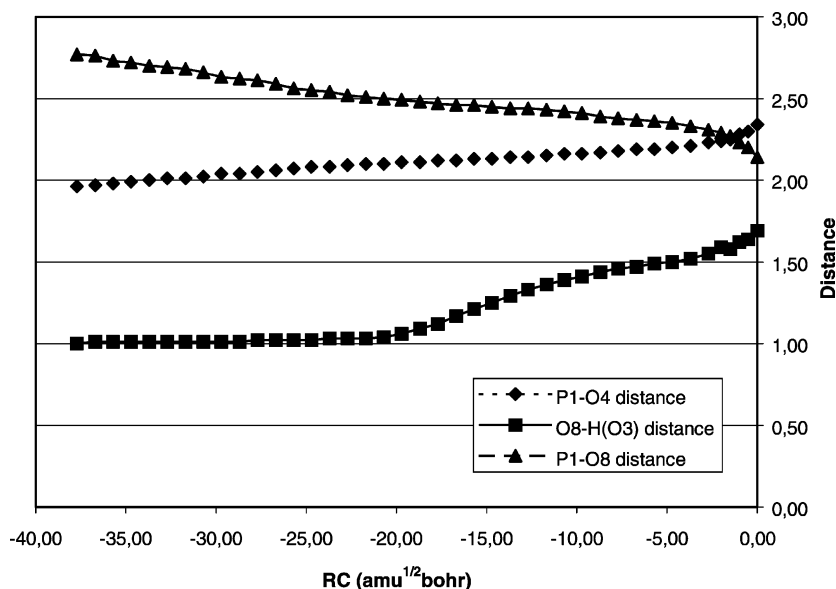


Fig. 2. IRC for reaction  $\text{MDP} + \text{H}_2\text{O} \rightarrow \text{MP} + \text{H}_2\text{P}$ . Changes in the P1–O4, O8–H(O3) and P1–O8 bond lengths (in Å) as a function of the reaction coordinate. Atoms are labeled according to Scheme 2. H(O3) refers to the H atom bonded to O3 in H2P.

$-12.50 \text{ kcal mol}^{-1}$ , due to the larger solvation energy of MDP ( $405.86 \text{ kcal mol}^{-1}$ ) compared to MP ( $-220.39 \text{ kcal mol}^{-1}$ ) and H2P ( $-61.99 \text{ kcal mol}^{-1}$ ). The computed activation energies in vacuum and water solution are  $8.89$  and  $36.43 \text{ kcal mol}^{-1}$ , respectively. The increase of activation energy observed in solvent originates again from solvation effects. In MDP-TS, the electron density is more evenly distributed than in MDP (see Tables 1 and 2), resulting in smaller solvation energy of the transition state.

Note that the activation energy for GTP hydrolysis has been estimated to be about  $30 \text{ kcal mol}^{-1}$  [26], in reasonable agreement with our results. In addition, our results show that GTP itself can act as the base catalyst in  $\text{H}_2\text{O}$  activation, in agreement with previous suggestions [23,24]. However, this does not exclude a role for Gln61 in the enzymatic system, whose presence is not modeled in the present investigation.

Once investigated MDP hydrolysis, we turned our attention to the corresponding  $\text{Mg}^{2+}$  complex

Table 1

Mulliken partial atomic charges of reactants, transition state and products for methyl-pyrophosphate hydrolysis in vacuum

Atom type and number	Reagents (MDP + H <sub>2</sub> O)	Transition state (MDP-TS)	Products (MP + H <sub>2</sub> P)
O1	-1.24	-1.14	-1.16
O2	-1.23	-1.15	-1.17
O3	-1.23	-1.07	-1.07
O4	-1.18	-1.18	-1.24
O5	-1.22	-1.23	-1.23
O6	-1.21	-1.23	-1.24
O7	-0.89	-0.88	-0.87
O8	-0.95	-1.14	-1.06
P1	+2.46	+2.46	+2.47
P2	+2.52	+2.48	+2.44

For the sake of clarity only relevant atoms, labeled according to Scheme 2, have been reported.

Table 2

Mulliken partial atomic charges of reactants, transition state and products for methyl-pyrophosphate hydrolysis in aqueous solution

Atom type and number	Reagents (MDP + H <sub>2</sub> O)	Transition state (MDP-TS)	Products (MP + H <sub>2</sub> P)
O1	-1.23	-1.15	-1.07
O2	-1.23	-1.16	-1.18
O3	-1.22	-1.07	-1.07
O4	-1.20	-1.21	-1.24
O5	-1.21	-1.23	-1.24
O6	-1.21	-1.23	-1.25
O7	-0.89	-0.90	-0.90
O8	-0.99	-1.14	-1.18
P1	+2.43	+2.43	+2.47
P2	+2.50	+2.45	+2.42

For the sake of clarity only relevant atoms, labeled according to Scheme 2, have been reported.

(hereafter referred as Mg-MDP; see Scheme 2b), to investigate the catalytic role of the metal ion. Indeed, it has been suggested that metal ion coordination to the  $\gamma$ -phosphoryl oxygen in GTP-Mg complexes

could increase the susceptibility of the phosphorus atom to nucleophilic attack and therefore increase the associative character of the transition state [27]. However, comparisons of linear free energy relationship

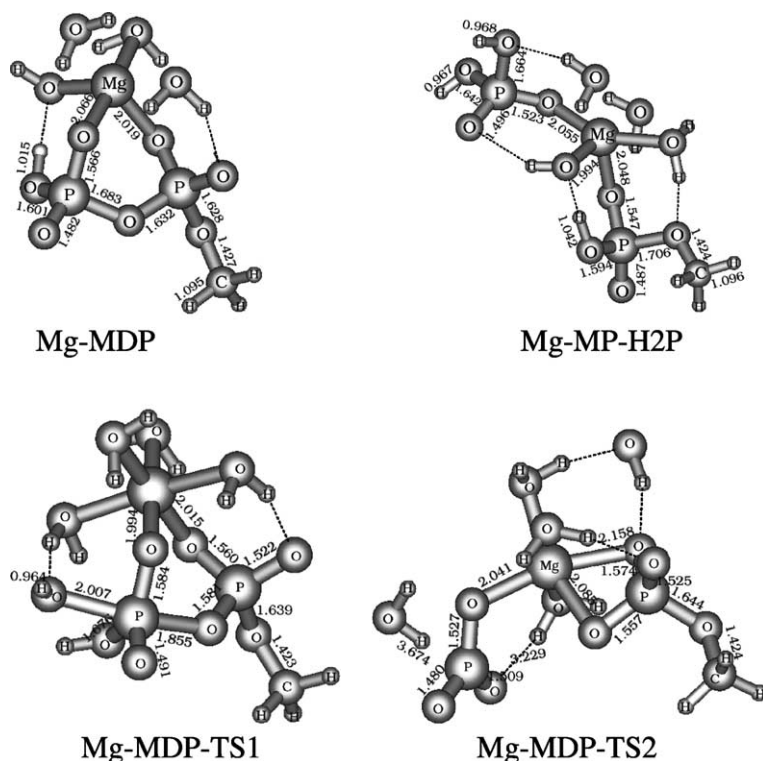


Fig. 3. DFT optimized structures of Mg-MDP, Mg-MP-H<sub>2</sub>P, Mg-MDP-TS1 and Mg-MDP-TS2. Relevant bond distances (in angstrom) are shown. X-ray derived [8] bond lengths for GTP are: P2–O7 = 1.61 Å, P2–O6 = 1.48 Å, P2–O5 = 1.48 Å, P2–O4 = 1.68 Å, P1–O4 = 1.70 Å, P1–O2 = 1.56 Å, P1–O1 = 1.47 Å, P1–O3 = 1.47 Å. Mg–O bonds are explicitly shown only when the Mg–O distance is lower than 2.2 Å. In any case, all oxygen atoms coordinated to Mg<sup>2+</sup> are within 2.32 Å from the metal ion, with the only exception of one water molecule in Mg-MDP-TS2 (see text). Hydrogen bonds are shown as dashed lines.

Table 3

Mulliken partial atomic charges of reactants, transition state and products for  $[\text{Mg}(\text{H}_2\text{O})_4(\text{P}_2\text{O}_7\text{CH}_3)]^{-1}$  hydrolysis in vacuum

Atom type and number	Reagents (Mg-MDP)	Mg-MDP-TS1	Mg-MDP-TS2	Products (Mg-MP-H2P)
Mg	+1.67	+1.68	+1.68	+1.68
O1	-1.10	-1.13	-1.00	-1.13
O2	-1.08	-1.04	-1.09	-1.03
O3	-1.29	-1.30	-1.19	-1.24
O4	-1.15	-1.14	-1.27	-1.11
O5	-1.15	-1.16	-1.15	-1.09
O6	-1.25	-1.29	-1.27	-1.28
O7	-0.84	-0.85	-0.85	-0.88
O8	-0.95	-1.11	-0.98	-1.05
O <sub>coord</sub>	-1.06	-1.03	-1.00	-1.04
O <sub>coord</sub>	-1.02	-1.04	-1.07	-1.05
O <sub>coord</sub>	-1.08	-1.10	-1.07	-1.24 <sup>a</sup>
O <sub>coord</sub>	-1.22 <sup>a</sup>	-1.11	-1.06	-1.05
P1	+2.58	+2.54	+2.39	+2.54
P2	+2.60	+2.60	+2.53	+2.56

For sake of clarity, only relevant atoms, labeled according to Scheme 2, have been reported. Oxygen atoms belonging to water molecules coordinated to  $\text{Mg}^{2+}$  are labeled O<sub>coord</sub>.

<sup>a</sup> Deprotonated water molecule.

for reaction of GTP and GTP-Mg did not confirm this hypothesis [28].

In Mg-MDP, the Mg ion has an octahedral geometry, being coordinated by four water molecules and two oxygen atoms belonging to  $\alpha$ - and  $\beta$ -phosphate (see Fig. 3). Remarkably, during the geometry optimization one  $\text{H}^+$  moved from a water molecule, whose acidity is increased by metal coordination,

to  $\beta$ -phosphate. Differently from MDP, the bond distances P1–O4 and P2–O4 in Mg-MDP are very similar (1.683 and 1.632 Å, respectively), due to the lower total charge (–1 versus –3) and to P–O bond polarization by  $\text{Mg}^{2+}$  (see Tables 1–4). Remarkably, computed bond distances and valence angles (data not shown) for Mg-MDP are very similar to the corresponding values obtained for GTP by X-ray

Table 4

Mulliken partial atomic charges of reactants, transition state and products for  $[\text{Mg}(\text{H}_2\text{O})_4(\text{P}_2\text{O}_7\text{CH}_3)]^{-1}$  hydrolysis in aqueous solution

Atom type and number	Reagents (Mg-MDP)	Mg-MDP-TS1	Mg-MDP-TS2	Products (MG-MP-H2P)
Mg	+1.67	+1.68	+1.68	+1.68
O1	-1.13	-1.17	-1.02	-1.15
O2	-1.09	-1.05	-1.08	-1.05
O3	-1.28	-1.29	-1.19	-1.26
O4	-1.15	-1.17	-1.28	-1.14
O5	-1.15	-1.17	-1.17	-1.10
O6	-1.25	-1.28	-1.27	-1.27
O7	-0.86	-0.86	-0.86	-0.89
O8	-0.99	-1.12	-0.99	-1.06
O <sub>coord</sub>	-1.07	-1.05	-1.02	-1.06
O <sub>coord</sub>	-1.04	-1.05	-1.08	-1.06
O <sub>coord</sub>	-1.07	-1.09	-1.07	-1.24 <sup>a</sup>
O <sub>coord</sub>	-1.25 <sup>a</sup>	-1.10	-1.06	-1.05
P1	+2.57	+2.54	+2.39	+2.54
P2	+2.59	+2.60	+2.53	+2.56

For the sake of clarity, only relevant atoms, labeled according to Scheme 2, have been reported. Oxygen atoms belonging to water molecules coordinated to  $\text{Mg}^{2+}$  are labeled O<sub>coord</sub>.

<sup>a</sup> Deprotonated water molecule.

diffraction (see Fig. 3), indicating that Mg-MDP may be considered a suitable model of GTP within the protein. The octahedral coordination environment of  $Mg^{2+}$  is maintained in the first reaction product (Mg-MP-H2P), where di-hydrogen-phosphate and methyl-phosphate are coordinated to the metal atom (see Fig. 3). Also in Mg-MP-H2P a proton has moved from a  $H_2O$  molecule coordinated to  $Mg^{2+}$  to a methyl-phosphate oxygen atom. The computed reaction energy for  $Mg-MDP + H_2O \rightarrow Mg-MP-H2P$  in vacuum is  $-15.59 \text{ kcal mol}^{-1}$ . The solvation energy differences between reagents and products are expected to be much smaller than those observed in the analogous reaction  $MDP + H_2O \rightarrow MP + H_2P$ , due to the lower total negative charge and the large (and comparable) size of reagents and products. In fact, the computed reaction energy in solution is  $-12.00 \text{ kcal mol}^{-1}$ .

For Mg-MDP hydrolysis, the sampling of the potential energy surface, carried out imposing slightly different starting structures in the synchronous transit quasi-Newton method [18], led to the characterization of two different transition states: one with an essentially associative character (Mg-MDP-TS1) and the other with dissociative character (Mg-MDP-TS2). In Mg-MDP-TS1, as in MDP-TS, the incoming water molecule is deprotonated and the  $OH^-$  group is the attacking nucleophile. However, in Mg-MDP-TS1, the  $H^+$  is transferred to the  $OH^-$  coordinated to  $Mg^{2+}$  and not to the  $\beta$ -phosphate group (that is already protonated in Mg-MDP and Mg-MDP-TS1), as observed in MDP-TS. The P1 atom has trigonal bipyramidal geometry, with longer P–O axial bonds ( $P1-O8 = 2.007 \text{ \AA}$ ,  $P1-O4 = 1.855 \text{ \AA}$ ). The comparison of these distances with the corresponding values computed for MDP-TS shows that  $Mg^{2+}$  coordination increases the associative character of the transition state. The activation energy computed in vacuum for Mg-MDP-TS1 ( $24.08 \text{ kcal mol}^{-1}$ ) is larger than the corresponding value obtained considering MDP hydrolysis ( $8.89 \text{ kcal mol}^{-1}$ ). However, as discussed above, computed energy values for the  $MDP + H_2O \rightarrow MP + H_2P$  reaction in vacuum are biased by the large total negative charge of MDP ( $-3$ ), which favor phosphoester bond cleavage. The comparison of activation energies computed considering solvent effects is more interesting and reveals the catalytic role of  $Mg^{2+}$  in promoting phosphoester

hydrolysis. In fact, the activation energy decreases by about one-half going from MDP ( $36.43 \text{ kcal mol}^{-1}$ ) to Mg-MDP ( $18.03 \text{ kcal mol}^{-1}$ ). The catalytic role of  $Mg^{2+}$  can be partly explained considering that the metal ion increases the electrophilicity of the phosphorous atoms P1, as deduced by comparison of its atomic charge values in MDP (2.43) and Mg-MDP (2.57), favoring the  $OH^-$  attack on P1. This observation and the lower total negative charge explain also the increased associative character of Mg-MDP-TS1 with respect to MDP-TS. Indeed, in an associative transition state electron density is expected to accumulate at the five-coordinated  $\beta$ -phosphate. However, analysis of Mg-MDP-TS1 partial atomic charges (Tables 3 and 4) shows that the increased electron density on  $\beta$ -phosphate is negligible, due to the buffering effect of the metal ion. In addition, the  $OH^-$  anion in Mg-MDP-TS1 is stabilized by a hydrogen bond with the coordinated water.

As stated above, we found also a transition state (Mg-MDP-TS2) characterized by dissociative character. In fact, in Mg-MDP-TS2,  $P1-O4$  and  $P1-O8$  distances are very large ( $3.229$  and  $3.674 \text{ \AA}$ , respectively). Remarkably, in Mg-MDP-TS2,  $Mg^{2+}$  is coordinated by the leaving oxygen atom O4 ( $Mg-O4 = 2.088 \text{ \AA}$ ), and releases a  $H_2O$  molecule from its coordination sphere. Moreover, in Mg-MDP-TS2, the proton bound to  $\beta$ -phosphate is transferred back to a water molecule, as expected considering the electronic properties of metaphosphate ( $PO_3^-$ ). In a dissociative transition state, negative charge is expected to accumulate at  $\alpha$ -phosphate. Thus, driving factors for GTP hydrolysis via a dissociative transition state are stabilization of  $\alpha$ -phosphate and weakening of the bond between  $\alpha$ - and  $\beta$ -phosphate. In fact, in Mg-MDP-TS2 the excess of negative charge on  $\alpha$ -phosphate is buffered by  $Mg^{2+}$  coordination (see Tables 3 and 4), explaining its catalytic role in a dissociative mechanism.

Considering the computed activation energies, it turns out that the dissociative mechanism is kinetically more favorable than the associative one, both in vacuum ( $6.25 \text{ kcal mol}^{-1}$ ) and in solution ( $11.22 \text{ kcal mol}^{-1}$ ). Also in this case solvation effects stabilize reagents with respect to transition state, due to larger size and smoother electron distribution in the latter (see Table 4).



## 4. Conclusions

In conclusion, the present DFT investigation of the phosphoester hydrolysis step carried out on GTP models has allowed a better definition of the catalytic role of  $Mg^{2+}$  ions in this biologically relevant reaction step. In particular, our results show that  $Mg^{2+}$  promotes both an associative mechanism, by increasing the electrophilicity of the reactive phosphorous atom, and a dissociative mechanism, favoring the P–O bond cleavage due to  $Mg^{2+}$ –O interaction. The observation that the dissociative mechanism is kinetically more favorable might be also relevant in light of the available information concerning the Ras enzymatic system whose molecular characteristics are not well suited for  $H_2O$  activation, due to the poor basic properties of the residues forming the active site [23,24]. Indeed, whereas  $H_2O$  activation is a key factor in an associative mechanism, it is less crucial in a dissociative mechanism, where the nucleophilicity of the attacking species does not play a significant role, suggesting that a dissociative mechanism for GTP hydrolysis is operative also when considering the enzymatic system.

## Supplementary materials

Graphical representations of the imaginary vibrational modes for the transition states are available from the authors upon request.

## References

- [1] F.H. Westheimer, *Science* 235 (1987) 1173.
- [2] G.R.J. Thatcher, R. Kluger, *Adv. Phys. Org. Chem.* 25 (1989) 99.
- [3] J. Florian, A. Warhel, *J. Phys. Chem. B* 102 (1998) 719.
- [4] N. Futatsugi, M. Hata, T. Hoshino, M. Tsuda, *Biophys. J.* 77 (1999) 3287.
- [5] M. Bianciotto, J.-C. Barthelat, A. Vigroux, *J. Am. Chem. Soc.* 124 (2002) 7573.
- [6] A. Cavalli, P. Carloni, *J. Am. Chem. Soc.* 124 (2002) 3763.
- [7] M.S. Boguski, E. McCormick, *Nature* 366 (1993) 643.
- [8] M.V. Milburn, L. Tong, A.M. DeVos, A. Brunger, Z. Yamaizumi, S. Nishimura, S.-H. Kim, *Science* 247 (1990) 939.
- [9] N. Strater, W.N. Lipscomb, T. Klabunde, B. Krebs, *Angew. Chem. Int. Ed. Engl.* 35 (1996) 2024.
- [10] D.E. Wilcox, *Chem. Rev.* 96 (1996) 2435.
- [11] N.H. Williams, *J. Am. Chem. Soc.* 122 (2000) 12023.
- [12] M. Cossi, V. Barone, R. Cammi, J. Tomasi, *J. Chem. Phys. Lett.* 255 (1996) 327.
- [13] A.D. Becke, *Phys. Rev. A* 38 (1988) 3098–3104.
- [14] A.D. Becke, *J. Chem. Phys.* 96 (1992) 2155.
- [15] A.D. Becke, *J. Chem. Phys.* 98 (1993) 5648.
- [16] P.J. Stevens, F.J. Devlin, C.F. Chabrowski, M.J. Frisch, *J. Phys. Chem.* 98 (1994) 11623.
- [17] H. Saint-Martin, L.E. Ruiz-Vicent, A. Ramirez-Solis, I. Ortega-Blake, *J. Am. Chem. Soc.* 118 (1996) 12167.
- [18] C. Peng, H.B. Schlegel, *Israel J. Chem.* 33 (1994) 449.
- [19] M.J. Frisch, G.W. Trucks, H.B. Schlegel, G.E. Scuseria, M.A. Robb, J.R. Cheeseman, V.G. Zakrzewski, J.A. Montgomery, R.E. Stratmann, J.C. Burant, S. Dapprich, J.M. Millam, A.D. Daniels, K.M. Kudin, M.C. Strain, O. Farkas, J. Tomasi, V. Barone, M. Cossi, R. Cammi, B. Mennucci, C. Pomelli, C. Adamo, S. Clifford, J. Ochterski, A. Petersson, P.Y. Ayala, Q. Cui, K. Morokuma, D.K. Malick, A.D. Rabuck, K. Raghavachari, J.B. Foresman, J. Cioslowski, J.V. Ortiz, B.B. Stefanov, G. Liu, A. Liashenko, P. Piskorz, R. Komaromi, R. Gomperts, R.L. Martin, D.J. Fox, T. Keith, M.A. Al-Laham, C.Y. Peng, A. Nanayakkara, C. Gonzales, M. Challacombe, P.M.W. Gill, B.G. Johnson, W. Chen, M.W. Wong, J.L. Andres, M. Head-Gordon, E.S. Replogle, J.A. Pople, *Gaussian98, Revision A.1*, Gaussian Inc, Pittsburgh, PA, 1998.
- [20] David R. Lide, *Handbook of Chemistry and Physics*, Chapman & Hall/CRC Press, London/Boca Raton.
- [21] A. Wittinghofer, E.F. Pai, *Trends Biochem. Sci.* 16 (1991) 382.
- [22] M. Frech, T.A. Darden, L.G. Pedersen, C.K. Foley, P.S. Charifson, M.W. Anderson, A. Wittinghofer, *Biochemistry* 33 (1994) 3237.
- [23] T. Schweins, M. Geyer, K. Scheffzek, A. Warshel, H.R. Kalbitzer, A. Wittinghofer, *Nat. Struct. Biol.* 2 (1995) 36.
- [24] T. Schweins, M. Geyer, H.R. Kalbitzer, A. Wittinghofer, A. Warshel, *Biochemistry* 35 (1996) 14225.
- [25] K.A. Maegley, S.J. Admiral, D. Herschlag, *Proc. Nat. Acad. Sci. U.S.A.* 93 (1996) 8160.
- [26] T.M. Glennon, J. Villa, A. Warshel, *Biochemistry* 39 (2000) 9641.
- [27] T. Schweins, R. Langen, A. Warshel, *Nat. Struct. Biol.* 1 (1994) 476.
- [28] S.J. Admiraal, D. Herschlag, *Chem. Biol.* 2 (1995) 729.